

Supporting Information

Short-Range Ordered-Disordered Transition of NiOOH/Ni(OH)₂ Pair Induces Switchable Wettability

Ya-Huei Chang,^a Nga Yu Hau,^a Chang Liu,^a Yu-Ting Huang,^a Chien-Cheng Li,^a Kaimin Shih,^b Shien-Ping Feng^{*,a}

Contents

(1) Supplementary Figures and Table

Figure S1. Plating profile of amorphous and nanoporous NiOOH.

Figure S2. Long-term stability and cycling test.

Figure S3. Roughness of FTO and stainless steel.

Figure S4. A photograph of shape deformation on rough SS before detachment, leading to the calculated adhesion force between the water droplet and Ni(OH)₂/SS of 33 μN.

Figure S5. Conventional XRD of as-prepared film and its exposure to high EC for 1 hr, and to UVO₃ for 10 mins.

Figure S6. (a) Ordered Ni-LDH, (b) turbostratic disordered Ni(OH)₂ and (c) short-range disordered Ni(OH)₂ where the basal planes face the air at a certain angle.

Figure S7. A photograph of the smiling pattern with wet eyes and mouth on a dry face.

Figure S8. (a) Cathodic waves of cyclic voltammetry for nickel. The inset is a photograph of the nickel strips. (b) Gold nanoparticles suspended on the scaffolds of hydrophobic Ni(OH)₂ at -2V.

Table S1. Summary of the O 1s peak fitting results for the O²⁻, OH⁻ and hydroscopic H₂O.

(2) Supplementary Videos

Video S2. The proof of good water-repellancy between the Ni(OH)₂/SS and the water droplet.

Video S3. The real-record of 2D microfluidic channels with optical microscopy.

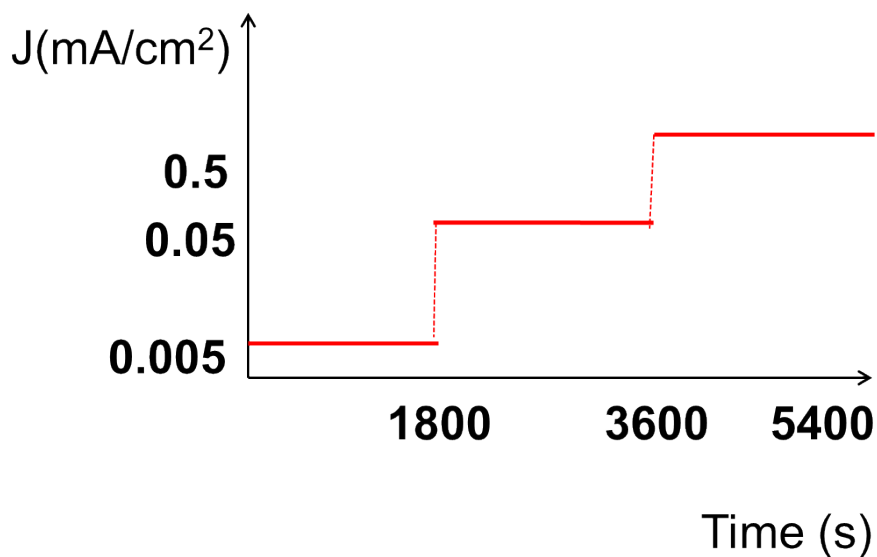


Figure S1. Plating profile of amorphous and nanoporous NiOOH.

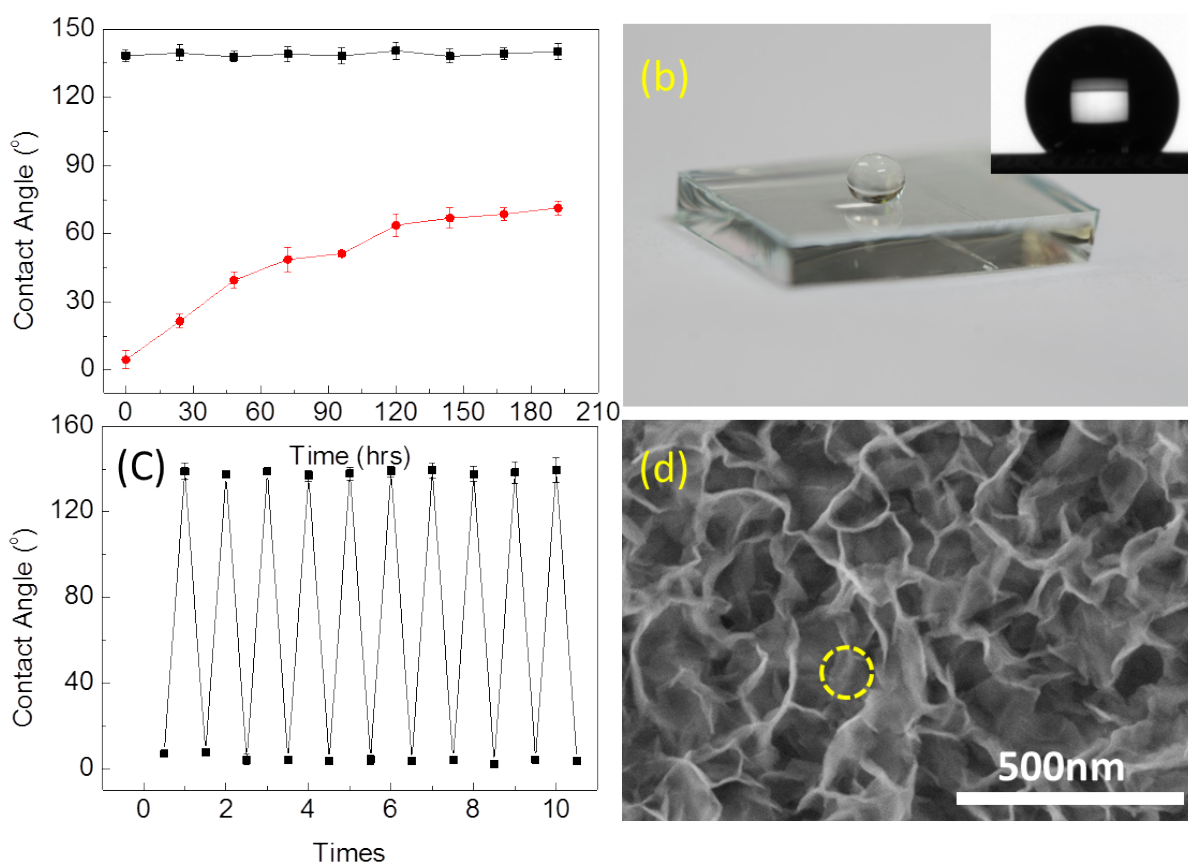


Fig. S2. (a) Long-term stability of wetting state (NiOOH/FTO) and dewetting state ((Ni(OH)₂/FTO) stored at ambient atmosphere during 8 days. (b) Dewetting state (Ni(OH)₂) stored at ambient atmosphere after 3 months. (c) Cycling test upon environmental chamber and UV/ozone alternatively. (d) FE-SEM image of hydrophobic Ni(OH)₂ film with micro-collapse after thermally cycling test.

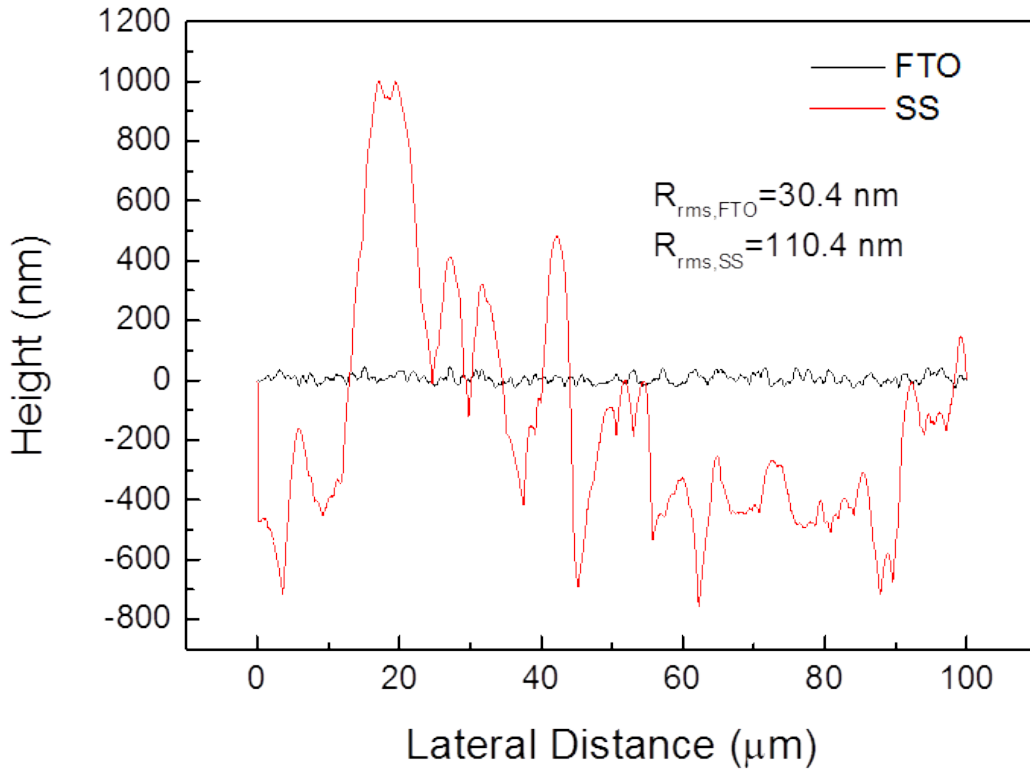


Figure S3. Roughness of FTO and stainless steel.



Figure S4. A photograph of shape deformation on rough SS before detachment, leading to the calculated adhesion force between the water droplet and Ni(OH)₂/SS of 33μN by balancing vertical forces, as shown in equation (S1)

$$f = \pi R_x \gamma \left(1 - \frac{R_x}{R_y} \right) - \rho V g \quad (S1)$$

where γ is surface tension of water. R_x and R_y are the principal radii of curvature. The last term represents the gravitational force acting on the lower part of the water droplet, where ρ and V are the density and volume of lower part of water droplet, and g is the gravitational acceleration.

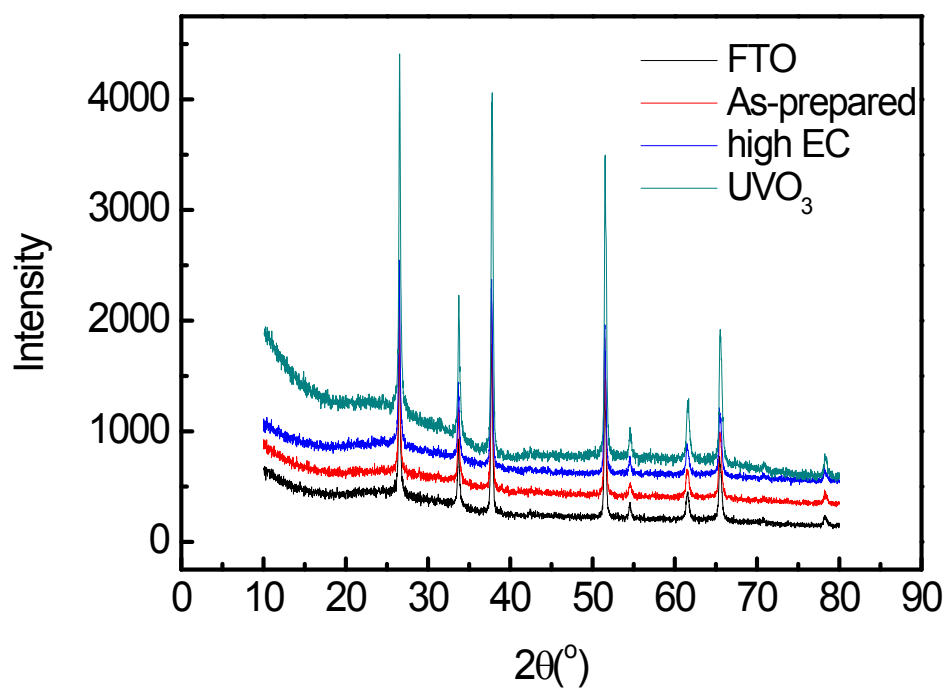


Figure S5. Conventional XRD of as-prepared film and its exposure to high EC for 1 hr, and to UVO_3 for 10 mins.

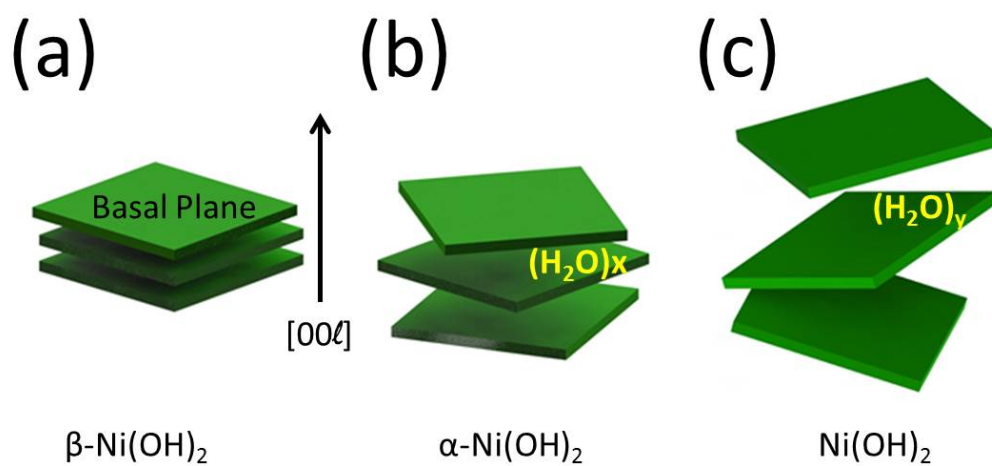


Figure S6. (a) Ordered Ni-LDH, (b) turbostratic disordered Ni(OH)_2 and (c) short-range disordered Ni(OH)_2 where the basal planes face the air at a certain angle.

Table S1. Summary of the O 1s peak fitting results for the O^{2-} , OH^- and hydroscopic H_2O .

Sample/Area	O^{2-}	OH^-	hydroscopic H_2O	O^{2-}/OH^-
As-prepared	22,480	23,286	4,642	0.97
High EC	0	45,120	0	0
UVO_3	11,273	35,344	5,532	0.32

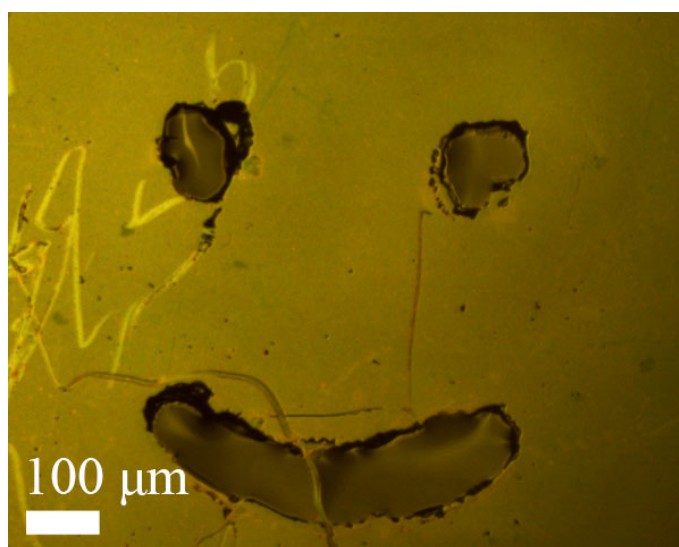


Figure S7. A photograph of the smiling pattern with wet eyes and mouth on a dry face.

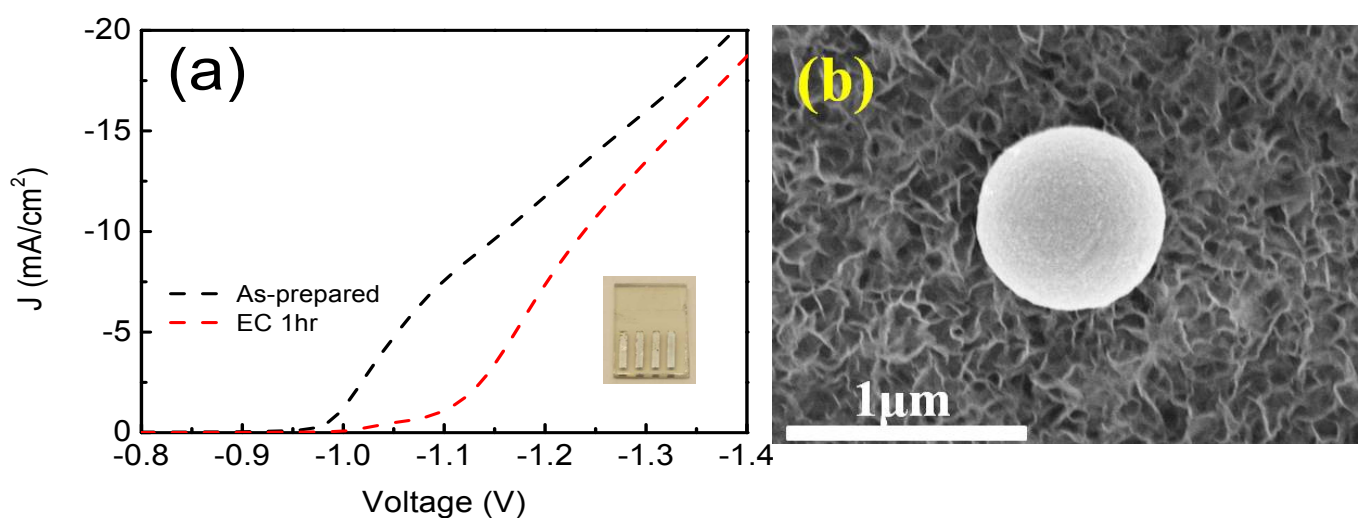


Figure S8. (a) Cathodic waves of cyclic voltammetry for nickel. The inset is a photograph of the nickel strips. (b) Gold nanoparticles suspended on the scaffolds of hydrophobic $Ni(OH)_2$ at -2V.